Metabolically Programmed Polyamine Analogue Antidiarrheals

Raymond J. Bergeron,* Guo Wei Yao, Hua Yao, William R. Weimar, Charles A. Sninsky,† Brian Raisler, Yang Feng, Qianhong Wu, and Fenglan Gao

Department of Medicinal Chemistry and College of Medicine, University of Florida, Gainesville, Florida 32610

Received November 9, 1995⊗

The design, synthesis, and testing of a novel class of antidiarrheal drugs based on a tetraamine pharmacophore are reported. While N^1,N^{14}-diethylhomospermine (DEHSPM) (5 mg/kg) completely prevents diarrhea in rodents, tissue distribution studies demonstrated that the principal metabolite of DEHSPM, homospermine (HSPM), accumulates and persists in tissues for a protracted period of time. This accumulation accounts for a large part of the chronic toxicity of DEHSPM. Thus a major objective was to develop a metabolically labile analogue of DEHSPM which retained the desirable biological properties of the parent drug. Hydroxyl groups, sites vulnerable to further metabolic transformation, were introduced into the external aminobutyl segments providing N^1,N^{14}-diethyl-(3*R*),(12*R*)-dihydroxyhomospermine [$(HO)_2$-DEHSPM]. The design concept was assisted by molecular modeling, which predicted that $(HO)_2$DEHSPM would have a K_i for polyamine transport essentially identical with that of DEHSPM. The experimentally measured K_i and also the observed values of other biological properties of $(HO)_2$DEHSPM were in fact identical with those of DEHSPM, including IC_{50} against L1210 cells, impact on the NMDA receptor, and impact on L1210 native polyamine pools. Most significantly, however, there was *no accumulation* of the dideethylated metabolite in tissues from mice treated chronically with $(HO)_2$DEHSPM, and $(HO)_2$DEHSPM was *3-fold less toxic than DEHSPM*. Finally, $(HO)_2$DEHSPM completely prevented diarrhea in the castor oil-treated rat model at a dose of 5 mg/kg, just as did DEHSPM.

Introduction

Gastrointestinal involvement frequently occurs in the course of human immunodeficiency virus (HIV) infection.[1] The etiology of AIDS-related diarrhea (ARD) is complicated and often difficult to assess and includes both enteric pathogens[2,3] and certain drugs.[4] Statistics show that about 50% of HIV patients in the United States will experience serious diarrhea during the course of their disease.[5,6] While a variety of treatment protocols have been attempted against various pathogens, the response is often only partial, and the relapse rate is very high.[7] Patients not only break through the therapeutic blanket, but even if the microorganism responds, an alternate pathogenic infection frequently develops.

Treatment options for ARD include the application of antimotility agents,[7] luminal-active agents,[7] or hormonal therapy.[3,8] Luminal-acting agents, generally either fibrous material or resins which absorb unbound bile acids, rarely provide any assistance in this disease. Antimotility agents, e.g., tincture of opium, morphine sulfate, and codeine, can be useful, although there are concerns with the addictive properties of these drugs.[7] Again, none of these agents is exceptionally effective in ARD. This may well be due to the fact that the problem has a large secretory component, very similar to that of cholera.[9]

Until recently octreotide was regarded as a potential solution to the problem. This somatostatin analogue, originally developed for diarrhea associated with vipomas, slows gastrointestinal transit and reduces secretory function. Results of a double blind study with this drug and ARD unfortunately were very disappointing.[10] Thus, identification of alternative effective antidiarrheals clearly represents a critical need in the care of patients with ARD. It has now become quite clear that polyamine analogues represent a serious therapeutic option for ARD, and clearly ARD is but one, albeit dramatic, of a number of clinical indications that would benefit from the development of potent new antidiarrheals.

In a series of elegant experiments, Tansy was able to demonstrate that polyamines have a pronounced effect on the motility of the gastrointestinal (GI) tract.[11] His original work focused on poly(ethyleneimine) and gastric emptying in rodents[12] and dogs.[13] Branched-chain poly(ethyleneimine)s effected significant inhibition of gastric emptying in rodents;[12] however, they caused a severe retch response in dogs.[13] Because of the structural relationship between the poly(ethyleneimine)s and natural polyamines, Tansy elected to evaluate the effect of spermidine and spermine and a group of polyamine analogues on the gastric emptying of rodents.[14] It soon became clear that polyamines had a profound influence on gastric emptying and that "endogenous spermine and spermidine may have some unrecognized GI secretomotor activity".[14] From a structure−activity perspective it also became obvious that very small changes in the polyamine's structure could completely eradicate the molecule's ability to inhibit gastric emptying. These studies strongly suggested that the polyamine pharmacophore was an excellent candidate for construction of antitransit, antidiarrheal drugs. Indeed this has now been demonstrated to be true.

Terminally diethylated homospermine, DEHSPM, a polyamine analogue designed and synthesized in these laboratories, is a very potent antidiarrheal.[15] This has been demonstrated in a number of animal models and recently in the clinic against ARD.[16] However, it does present with some troublesome metabolic properties in

† College of Medicine.

⊗ Abstract published in *Advance ACS Abstracts,* May 15, 1996.

S0022-2623(95)00827-2 CCC: $12.00

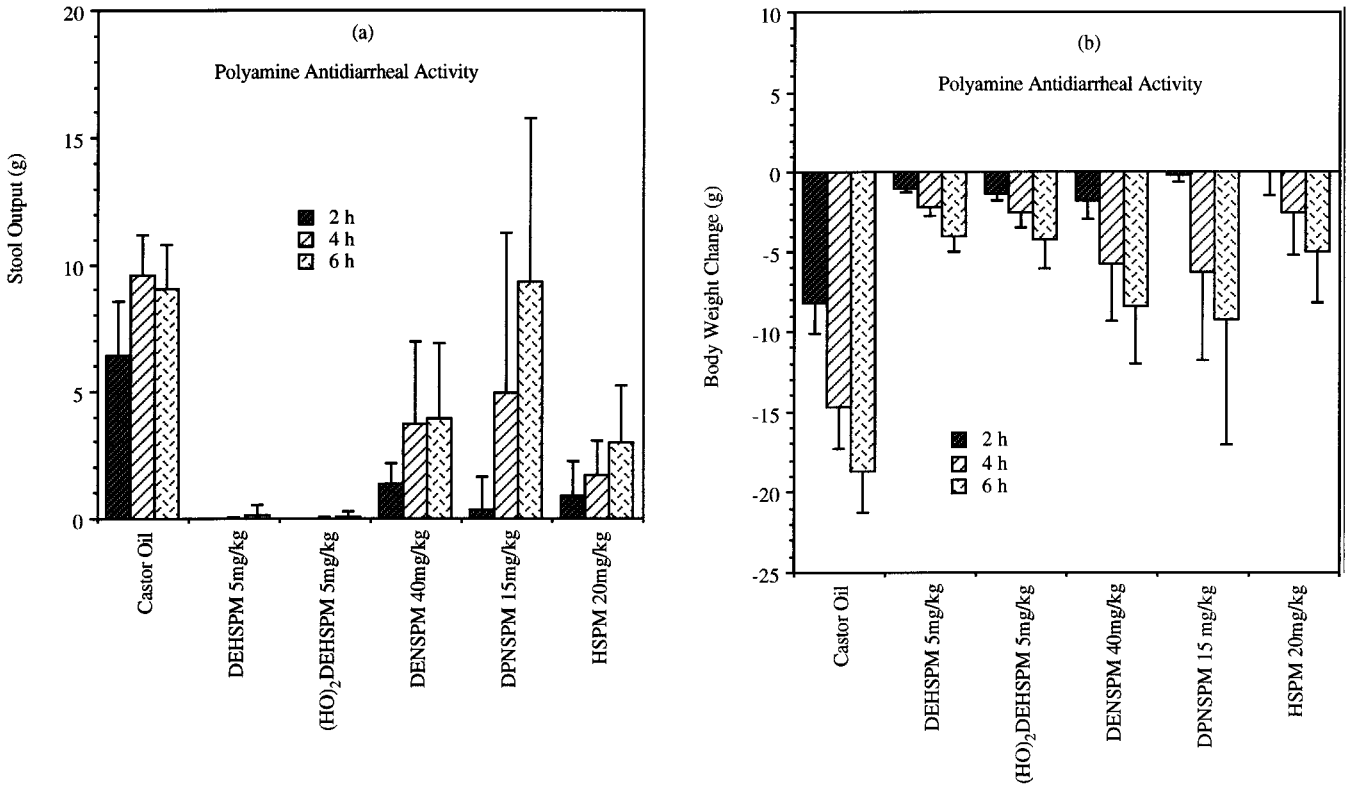

Figure 1. Antidiarrheal activity of polyamine analogues DENSPM, DPNSPM, HSPM, DEHSPM, and $(HO)_2$DEHSPM. All drugs were administered as an sc injection followed, after 30 min, by gastric gavage of castor oil (5 mL/kg). Stool output (a) and body weight loss (b) were measured at 2, 4, and 6 h. Both DEHSPM- and $(HO)_2$DEHSPM-treated rats showed virtually no stool output and lost little of their body weight as compared to castor oil control rats. HSPM-, DPNSPM-, and DENSPM-treated rats all became diarrheal during the 6 h assay. Data are not corrected for slight evaporative losses that occur during the assay. Such corrections do not significantly affect the results.

animals. DEHSPM is *N*-deethylated to homospermine (HSPM), which has a very protracted half-life, 2−3 weeks in mice and even longer in the dog.[17] Thus each subsequent dose of DEHSPM results in a further accumulation of HSPM until toxic levels of the parent tetraamine are reached. The current study is aimed at the design, synthesis, and testing of an antidiarrheal DEHSPM derivative into which we incorporate metabolically labile sites in the tetraamine backbone to ensure that such toxic tetraamines cannot accumulate, i.e., a metabolically programmed drug.

Results

Design Concept. The purpose of the initial antidiarrheal studies with the polyamine analogues was to assess which polyamine pharmacophore backbone was suitable for the development of antidiarrheals. Four compounds were evaluated as follows: homospermine (HSPM), N^1,N^{14}-diethylhomospermine (DEHSPM), N^1,N^{11}-diethylnorspermine (DENSPM), and N^1,N^{11}-dipropylnorspermine (DPNSPM). The antidiarrheal activity of the polyamine analogues was measured in a castor oil-induced diarrhea model in rats.

In the case of norspermines, neither of the compounds was an active antidiarrheal. DPNSPM at 15 mg/kg and DENSPM even at 40 mg/kg did not demonstrate any significant activity. When rodents were treated with 5 or 20 mg/kg HSPM, no significant antidiarrheal activity was observed. However, when animals were administered 5 mg/kg DEHSPM, there was an overall 100% reduction in stooling relative to castor oil controls (Figure 1a). Not surprisingly animal weight loss paralleled stool output (Figure 1b). We are currently and successfully treating patients with ARD with 30 mg/m^2 DEHSPM, the equivalent of 5 mg/kg in the rat. However, a problem associated with buildup and retention of its metabolite, HSPM, in tissues needed to be addressed.

In order to understand the buildup of the HSPM in DEHSPM-treated animals, we will briefly summarize our extensive metabolic studies on DEHSPM[17] and DENSPM.[18] While a number of the pharmacokinetic parameters of DEHSPM and DENSPM were similar, the metabolic profiles are very different. Although DENSPM and its metabolites were found in all tissues examined in mice treated with the drug, the liver and kidney had the highest level of metabolites. These catabolic products included N^1-ethylnorspermine (MENSPM), N^1-ethylnorspermidine (MENSPD), N^1-ethyl-1,3-diaminopropane (MEDAP), and norspermidine (NSPD), suggesting that DENSPM is metabolized (Figure 2) by (1) *N*-deethylation and (2) stepwise removal of 3-aminopropyl equivalents by spermine/spermidine N^1-acetyl transferase (SSAT)/polyamine oxidase (PAO), a metabolic pathway unique to the polyamines.[18] Five days after the end of a 6 day DENSPM treatment schedule, essentially all of the drug and metabolites had cleared the tissues.

In the case of DEHSPM, again the liver and kidney had the highest concentration of drug and its metabolites, N^1-ethylhomospermine (MEHSPM) and HSPM. The data clearly showed that as with DENSPM, *N*-deethylation is a key metabolic step in processing DEHSPM (Figure 3), but, that unlike NSPM, HSPM does not undergo further metabolism. As pointed out above, normal polyamine catabolism involves stepwise

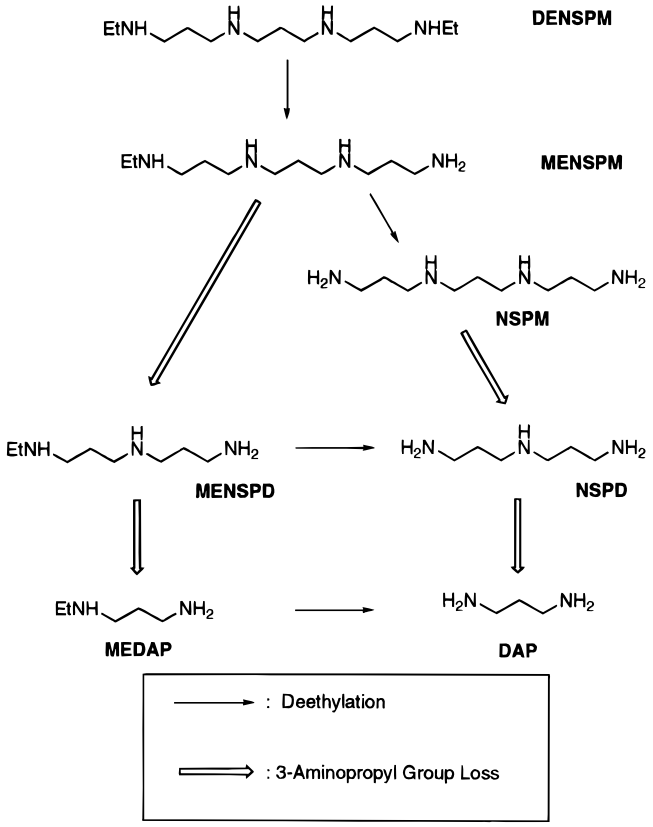

Figure 2. Metabolic breakdown (catabolism) of DENSPM. Two enzymatic systems are operative: (a) *N*-deethylation (solid arrows) and (b) de-3-aminopropylation (open arrows) by the constituitive system for catabolism of native polyamines, SSAT/PAO. The various permutations of these enzymatic reactions are shown, and each of the possible metabolites indicated in the figure was in fact observed in tissues of DENSPM-treated mice.[18]

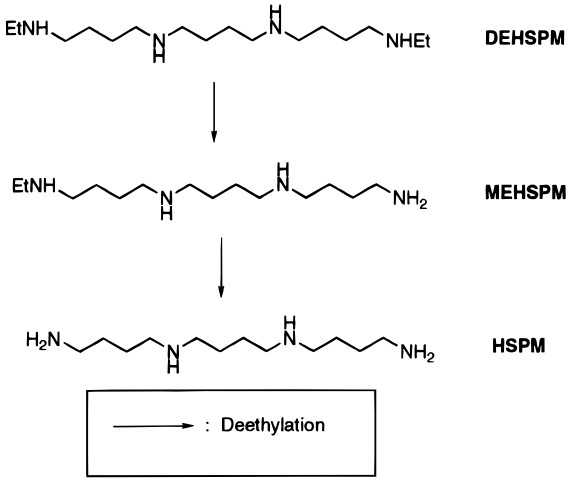

Figure 3. Catabolism of DEHSPM. Only the *N*-deethylation pathway is operative; the terminal 4-aminobutyl segments of HSPM are not recognized by SSAT/PAO, so that further degradation does not occur.

removal of aminopropyl equivalents by SSAT/PAO. In this pathway only primary 3-aminopropyl nitrogens are acetylated, and since HSPM has only 4-aminobutyl fragments, it cannot be processed. The accumulation and persistence of HSPM in the tissues of DEHSPM-treated animals are especially striking. One day after a 6 day treatment schedule of DEHSPM, a regimen identical with that of DENSPM, 35% of the drug administered to mice remains in the liver and kidney as drug or metabolites. Interestingly 84% of the drug remaining in the animal at this time is in the form of HSPM. By 5 days after the end of DEHSPM treatment, essentially no DEHSPM remains in the form of the parent drug, yet about 25% of the total dose is present as HSPM. It is quite clear that the increased chronic toxicity of DEHSPM over DENSPM is related to the buildup of HSPM.[17] The chronic toxicity of HSPM is 5 times greater than that of NSPM. Interestingly the chronic LD_{50} of DEHSPM is almost the same as that of HSPM and 5 times greater than that of DENSPM.

The key to a less toxic DEHSPM-like antidiarrheal is one in which the metabolite can be cleared from the tissues. Again because of the aminobutyl fragments of HSPM, this metabolite cannot be processed through the polyamine biosynthetic network; thus, it remains in the tissues for protracted periods of time. Neither the primary nor the secondary nitrogens of HSPM offer an opportunity for facile conversion to an easily cleared metabolite. Certainly the methylene backbones cannot be easily oxidized to an excretable metabolite. We thus elected to raise the oxidation state of two of the methylene groups of DEHSPM by introducing a single hydroxyl in the *R*-configuration at each of the external aminobutyl fragments, resulting in N^1,N^{14}-diethyl-(3*R*),(12*R*)-dihydroxyhomospermine, [$(HO)_2$DEHSPM] (**7**), Scheme 1. This offered potential sites for either conjugation (e.g., glucuronidation) or further oxidation and clearance.

Computer Modeling. The potential of comparative molecular field analysis (CoMFA) as a predictive tool in identifying analogues which would likely be successful as antidiarrheals has now been demonstrated. CoMFA is a relatively new technique used to correlate receptor−ligand affinities with the molecular, steric, and electrostatic fields presented by the ligands. The output of these studies is an interactive 3D color contour plot from which one can deduce which structural modifications are likely to improve activity.[19] Thus, the approach allows one to predict the activity of new structures which have not been synthesized and are not part of the model data set. Preliminary studies suggest this is a very useful tool in polyamine analogue design. As part of a National Cancer Institute-sponsored program focused on the development of polyamine analogues as antineoplastics, we have already applied the method to search for a quantitative relationship between structure and the ability of the analogue to compete with spermidine for the polyamine transport apparatus, K_i values. The initial quantitative structure−activity relationship (QSAR) CoMFA included 26 polyamine analogues and provided a model with a cross-validated $r^2 = 0.697$ (optimum components five) and the conventional $R^2 = 0.973$, F test = 152.726, $S = 0.143$.[20−22] The molecular modeling shows that the relative contributions of the steric and electrostatic terms in the QSAR equation are 0.673 and 0.327, respectively, specifying the importance of the geometry of the groups fixed to the nitrogen and of charge.

The library of compounds includes both linear analogues and the cyclic dipiperidyl and dipyridyl compounds along with N^1,N^{12}-bis(2,2,2-trifluoroethyl)spermine (FDESPM). The program was presented with a group of tetraamines in which the nitrogens were both charged and uncharged at physiological pH; thus it was able to assess the contribution of charge to K_i data

Table 1. Comparison of Experimental and Predicted K_i Values of Tetraamine Analogues Using CoMFA Models

Structure	Abbreviate	K_i (μM) Actual[a]	Calcd
Norspermines			
9 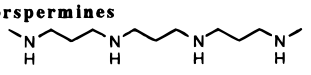	DMNSPM	5.6	5.9
10 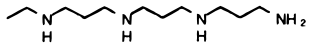	MENSPM	7.7	7.9
11 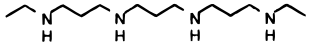	DENSPM	17	13.2
12 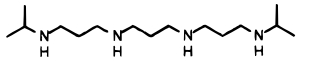	DIPNSPM	40	40.7
Spermines			
13 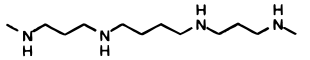	DMSPM	1.1	1.1
14 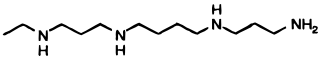	MESPM	1.7	1.1
15 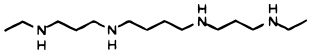	DESPM	1.6	2.0
16 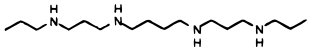	DPSPM	2.3	2.2
17 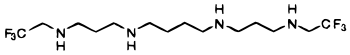	FDESPM	285	316
Homospermines			
18 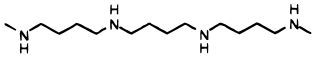	DMHSPM	0.97	1.6
19 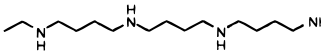	MEHSPM	1.1	1.3
20 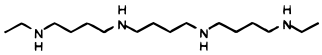	DEHSPM	1.4	1.9
21 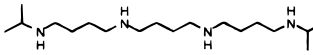	DIPHSPM	8.1	8.7
22 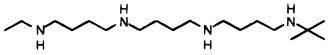	ETBHSPM	3	4.7
23 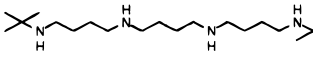	DTBHSPM	56	37.2
Homospermine homologues			
24 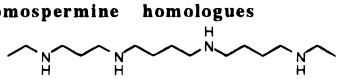	DE(3,4,4)	8	3.2
25 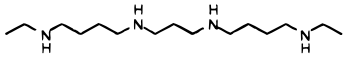	DE(4,3,4)	4	3.7
26 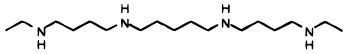	DE(4,5,4)	6.0	5.8
Piperidine and Pyridine Derivatives			
27 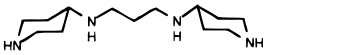	PIP(3,3,3)	60.5	69.2
28 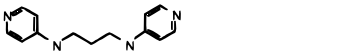	PYR(3,3,3)	>500	426
29 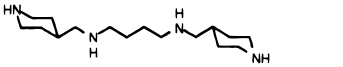	PIP(4,4,4)	4.9	4.9
30 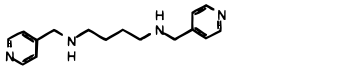	PYR(4,4,4)	>500	562
31 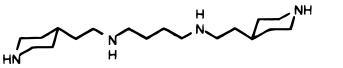	PIP(5,4,5)	18.1	17.0
Cyclohexane Derivatives			
32 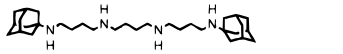	BAHSPM	2	3.2
33 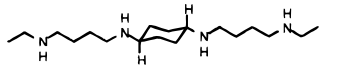	CHX(4,4,4)-trans	3.5	4.9
34 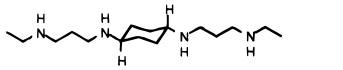	CHX(3,4,3)-trans	7.9	8.3

[a] Competitive inhibition of radiolabeled spermidine uptake in L1210 cells [K_m(SPD) = 2.1 ± 0.2 μM]. These values[29,30] represent the mean of at least three such experiments with a standard deviation typically about 10%.

(Table 1). Prior to embarking on the synthesis of $(HO)_2$-DEHSPM, we "asked" the computer to predict the K_i value. SYBYL suggested that $(HO)_2$DEHSPM should be recognized by the polyamine transport apparatus as effectively as DEHSPM with nearly identical calculated K_i values of 2.0 and 1.9 μM, respectively. The agreement between the actual K_i values was also outstanding, 1.8 vs 1.4 μM, respectively (Table 2).

In this regard we elected to assess how effective a K_i value would be in projecting the compound's IC_{50} values against L1210 cells, its impact on polyamine pools, its effect on the NMDA receptor, and most importantly its antidiarrheal activity. *A prori* one could not anticipate any quantitative relationship between competition for the polyamine transport apparatus and any of these other biological properties. However, perhaps it is not unreasonable to expect that if two molecules are recognized by this transport apparatus as being structurally similar, i.e., close in K_i values, it would not be surprising to see they have similar pharmacological properties in several areas.

Synthesis

The synthesis of polyamines $(HO)_2$DEHSPM (**7**) and (3*R*),(12*R*)-dihydroxyhomospermine [$(HO)_2$HSPM] (**8**), which contain chiral alcohols on the outer methylene chains, was accomplished by our methodology used to make hypusine.[23] *N*,*N*′-Dibenzylputrescine (**1**)[24] added regiospecifically to (*S*)-(+)-epichlorohydrin (2 equiv) to form (*S*,*S*)-bis-chlorohydrin **2** (Scheme 1). Treatment of **2** with KCN in the presence of 18-crown-6 gave dinitrile **3**, in which the alcohols are in the *R*-configuration. The cyano groups of **3** were hydrogenated with Raney nickel in methanolic ammonia resulting in primary α,ω-diamine **4**. Hydrogenolysis of the *N*-benzyl protecting groups of **4** under mild conditions (1 atm, 10% Pd−C, methanol, 4 equiv of HCl) furnished $(HO)_2$HSPM (**8**) as its tetrahydrochloride salt. Compound **4** was also converted to its tetraacetyl derivative **5** with acetic anhydride in methylene chloride. Exposure of **5** to $LiAlH_4$ in THF simultaneously reduced the acetamides to ethylamines and unmasked the secondary carbinols generating tetraalkylated polyamine **6**. Catalytic removal of the benzyl protecting groups of **6** over Pd−C in ethanolic HCl afforded terminally diethylated homospermine *R*,*R*-diol **7** as its tetrahydrochloride salt.

Biological Studies

IC_{50} for L1210 Cell Growth. While $(HO)_2$DEHSPM is more highly substituted than DEHSPM, it nevertheless maintains enough structural similarity to be "read" by L1210 cells as DEHSPM. The 48 and 96 h IC_{50} values of $(HO)_2$DEHSPM vs DEHSPM are very similar

Scheme 1. Synthesis of N^1,N^{14}-Diethyl-(3*R*),(12*R*)-dihydroxyhomospermine [$(HO)_2$DEHSPM] (**7**) and (3*R*),(12*R*)-Dihydroxyhomospermine [$(HO)_2$HSPM] (**8**)[a]

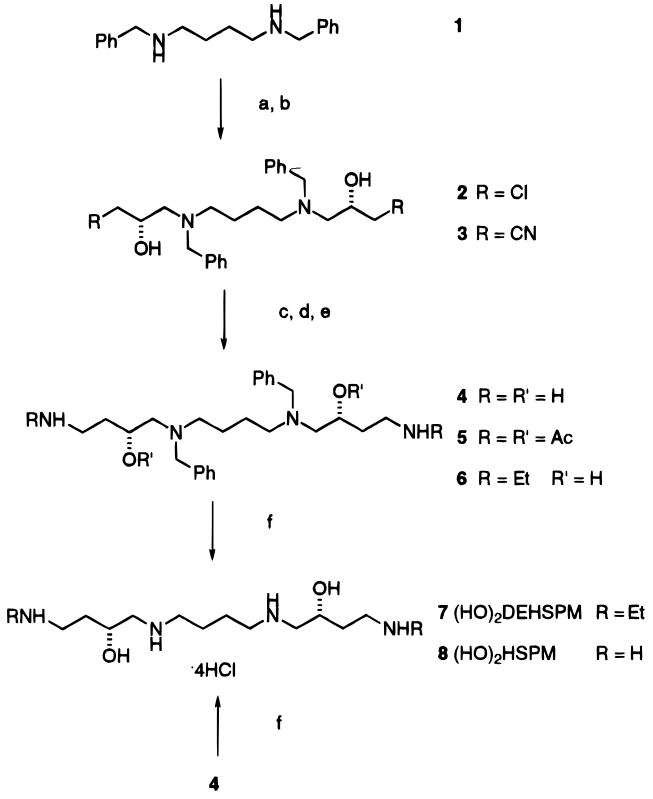

[a] Reagents: (a) (*S*)-(+)-epichlorohydrin/$MgSO_4$/MeOH; (b) KCN/18-crown-6/CH_3CN; (c) H_2/Ra Ni/NH_3/MeOH; (d) Ac_2O/CH_2Cl_2; (e) $LiAlH_4$/THF; (f) H_2/10% Pd−C/MeOH or EtOH/HCl.

Table 2. Analogue Structures, Acronyms, L1210 Growth Inhibition, and Effects on [^{3}H]Spermidine Transport

Structure	Acronym	IC_{50} (μM) 48 h	96 h	K_i[a] (μM)
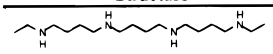	DEHSPM	0.2	0.05	1.4
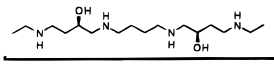	$(HO)_2$DEHSPM	0.6	0.05	1.8

[a] The K_i values were estimated from Lineweaver-Burke plots, which showed simple substrate-competitive inhibition of radiolabeled spermidine transport in L1210 cells. The V_{max} was typically about 1 nmol/h/10^6 cells; K_m(SPD) = 2.1 ± 0.2 μM.

(Table 2). In fact the actual 48 and 96 h IC_{50} curves for DEHSPM and $(HO)_2$DEHSPM are nearly identical (see Figure 4 for 96 h curves).

K_i Studies. The ability of $(HO)_2$DEHSPM and DEHSPM to compete with [^{3}H]spermidine for uptake into L1210 cells *in vitro* is very similar, with K_i values of 1.8 and 1.4 μM, respectively (Table 2).

Polyamine Pools. When L1210 cells were grown in 10 μM DEHSPM (K_i = 1.4 μM) for 48 h, they achieved an intracellular concentration of 2.9 mM DEHSPM. At 0.7 μM $(HO)_2$DEHSPM (0.4K_i) for 48 h, the concentration of intracellular drug reached 1.3 mM, while in 3.5 μM $(HO)_2$DEHSPM (2K_i), intracellular level of analogue reached 2.7 mM, almost identical with the intracellular DEHSPM concentration. At this essentially equimolar intracellular concentration, each analogue had the same impact on polyamine pools. Putrescine and spermidine were depleted to below detectable limits, while spermine was reduced to about 60% of control values (Table 3).

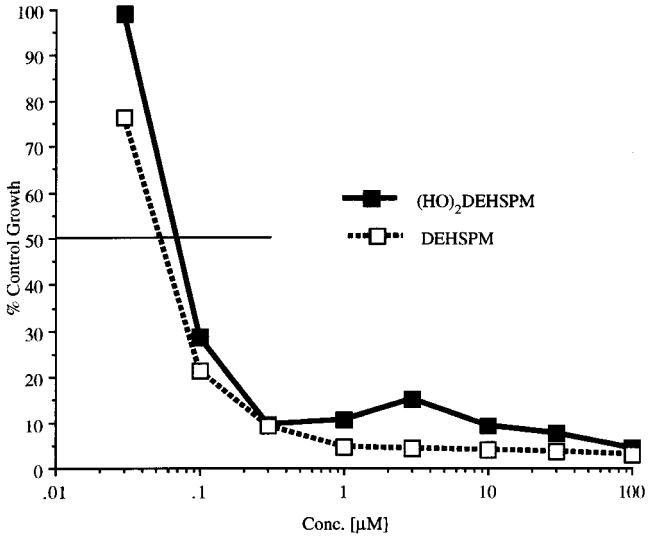

Figure 4. Comparison of the effects of DEHSPM and $(HO)_2$DEHSPM on L1210 cell 96 h growth curves. The concentration of drug that results in 50% inhibition of cell growth, i.e., the IC_{50}, is between 0.05 and 0.09 μM for DEHSPM and $(HO)_2$DEHSPM as indicated by the intersection of the '50% growth line' with the respective curves.

Table 3. Impact of Polyamine Analogues on Polyamine Pools[a]

compd	concn (μM)	PUT	SPD	SPM	analogue[b]
DEHSPM	10	0	0	61	2.94
$(HO)_2$DEHSPM	0.7	45	57	96	1.32
$(HO)_2$DEHSPM	3.5	0	0	68	2.73

[a] Native polyamine levels in analogue-treated L1210 cells are relative to untreated controls (control = 100%). Typical control values in pmol/10^6 L1210 cells are PUT = 192 ± 38, SPD = 2751 ± 163, and SPM = 726 ± 34. [b] Analogue amount is expressed as nmol/10^6 cells. Untreated L1210 cells (10^6) correspond to about 1 μL volume; therefore, concentration can be estimated as nmol/10^6 cells → mmol/L → mM. Treatment with polyamine analogues generally causes a shrinkage of L1210 cell volume dependent on time of exposure.[30]

Modulation of [^{3}H]MK-801 Binding to the NMDA Receptor by $(HO)_2$DEHSPM. The retention of certain characteristic pharmacological properties of the DEHSPM pharmacophore by $(HO)_2$DEHSPM is clearly exemplified in Figure 5. We have previously reported the marked activity of terminally dialkylated tetraamines including DEHSPM on the NMDA receptor and have shown that very small structural changes *can* result in striking differences in this activity among polyamine analogues.[25] The dose−effect curves of DEHSPM and $(HO)_2$DEHSPM are virtually superimposable. Agonist activity occurs at 0.5−1.0 μM, but marked antagonist activity is observed at concentrations above 5 μM with maximal antagonism at concentrations of 50 μM and above for both polyamines.

Metabolism of $(HO)_2$DEHSPM vs DEHSPM in Mouse Liver and Kidney. Dansylated samples of authentic $(HO)_2$DEHSPM or $(HO)_2$HSPM resulted in a single fluorescent peak in the HPLC with a molar response similar to that of DEHSPM or HSPM. Dansylation of the $HClO_4$ extracts of $(HO)_2$DEHSPM-treated liver and kidney contained the peaks corresponding to the natural polyamines, PUT, SPD, and SPM as well as unchanged $(HO)_2$DEHSPM. In addition there was a single additional fluorescent peak with a retention time identical with that of authentic dansylated $(HO)_2$HSPM. We were unable to identify a peak in the area in which we would anticipate the dansylated monodeethylated metabolite of $(HO)_2$DEHSPM. How-

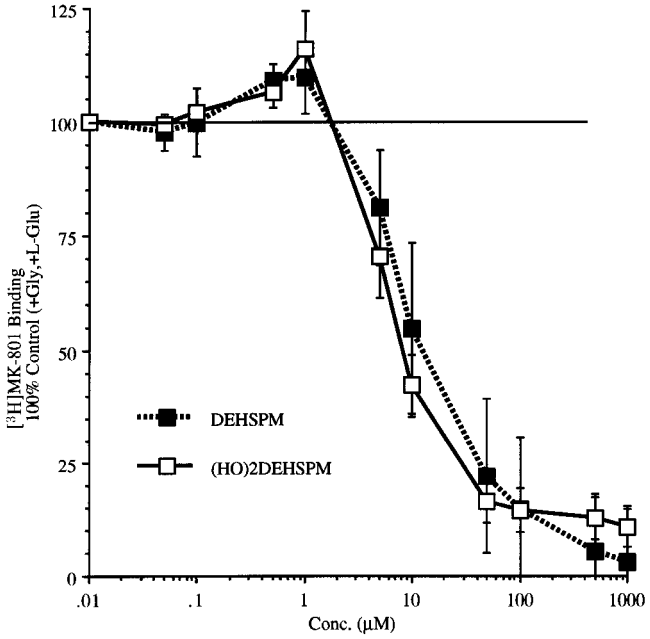

Figure 5. Effects of $(HO)_2$DEHSPM and DEHSPM on NMDA receptor (MK-801) binding. Each data point represents the mean ± SD of three experiments. Each experiment was in turn performed in triplicate; "100%" activity is defined as the amount of specific MK-801 binding to washed rat cerebral cortical membranes in the presence of saturating concentrations of coagonists (100 μM L-glutamate, 100 μM glycine) and 2 nM [^{3}H]MK-801.

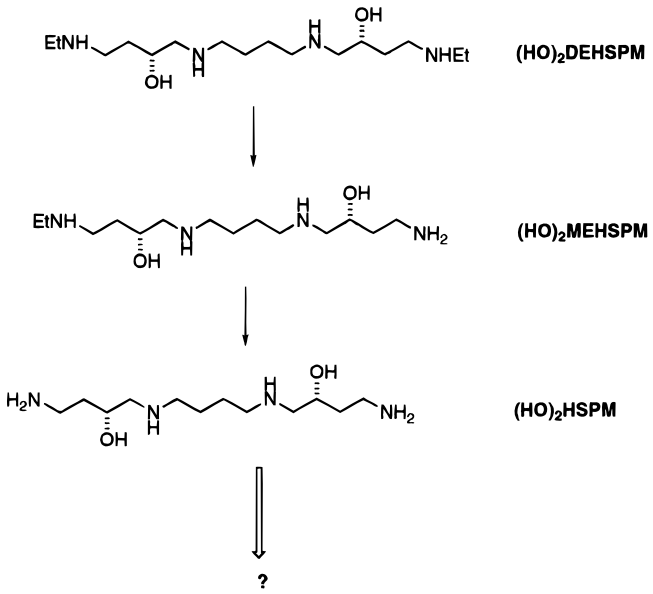

Figure 6. Proposed catabolism of $(HO)_2$DEHSPM. The *N*-deethylation pathway is operative as with DEHSPM, but in contrast to DEHSPM, the terminal 2-hydroxy-4-aminobutyl segments of $(HO)_2$HSPM are further degraded by other, yet to be characterized, enzymatic systems. Thus the metabolite $(HO)_2$HSPM does not accumulate.

ever without an authentic sample of this metabolite, it is not clear that its dansylated derivative is not buried under other signals. This remains to be established. Nevertheless it is clear that the initial step in $(HO)_2$-DEHSPM metabolism involves simple deethylation (Figure 6) as with DEHSPM.

It appears that the initial steps in the tissue distribution and metabolism of $(HO)_2$DEHSPM are indistinguishable from DEHSPM. The levels of unmetabolized drug present in liver and kidney 1 day after cessation of a subchronic equimolar treatment regimen are similar for $(HO)_2$DEHSPM and DEHSPM. In the liver the level of unchanged drug is similar and low: 83.6 ± 11.7 vs 43.9 ± 12.6 nmol/g of wet weight for $(HO)_2$DEHSPM and DEHSPM, respectively (Figure 7a). Levels in the kidney are also similar, though substantially higher than those in the liver: 481 ± 46 [$(HO)_2$DEHSPM] vs 409 ± 178 [DEHSPM] (Figure 7b). However, there is no substantial accumulation of metabolic products of $(HO)_2$DEHSPM in either tissue. This is in marked contrast with DEHSPM, in which tissues from treated animals contained the dideethylated metabolite HSPM in substantially higher concentrations than the parent drug. Thus HSPM is present in large quantities in the DEHSPM-treated liver (525 ± 44 nmol/g of wet weight) and at even higher levels in the kidneys, where it is easily the most abundant polyamine in the tissue (815 ± 61 nmol/g of wet weight), equivalent to all the other polyamines *combined*. The corresponding dideethylated metabolite $(HO)_2$HSPM is, in contrast, present in both liver (63 ± 2 nmol/g of wet weight) and kidney (63 ± 9 nmol/g of wet weight) but in concentrations lower than the parent drug (liver, 84 ± 12 nmol/g of wet weight; kidney, 481 ± 46 nmol/g of wet weight). The conse-

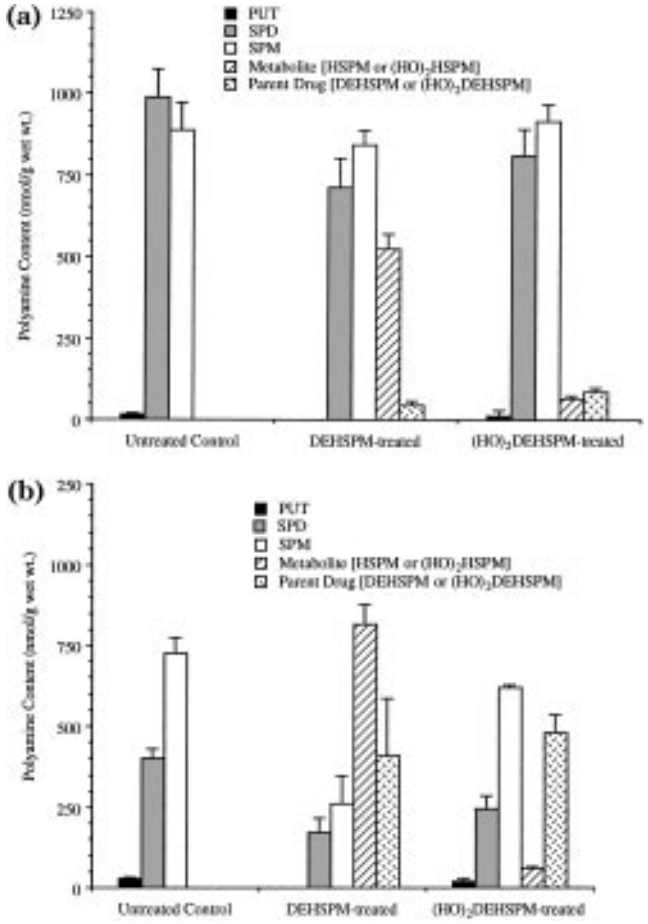

Figure 7. Quantitation of parent drug, $(HO)_2$DEHSPM, dideethylated metabolite, $(HO)_2$HSPM, and native polyamine pools in mouse liver (a) and kidney (b). Groups ($N = 3$; ±SD) were sacrificed for HPLC analysis 24 h after cessation of a subchronic dosage regimen (20 mg/kg/day $(HO)_2$DEHSPM as a single ip injection daily for 5 days; total dose = 3.0 mg or 6.46 μmol for a 30 g mouse). For comparison, similar data for untreated control and DEHSPM-treated (received "equimolar" subchronic dose of DEHSPM = 2.7 mg or 6.25 μmol for a 30 g mouse) mice are plotted. Total polyamine N^+ equivalents ± SD (nequiv × 10^{-1}/g of wet wt) for these tissues are calculated and given in Table 4.

Table 4. Effects of Chronic $(HO)_2$DEHSPM/DEHSPM Treatment on Polyamine Homeostasis

tissue		untreated control	$(HO)_2$DEHSPM[a]	DEHSPM[b]
liver	native [N^+]	6552 ± 609	6118 ± 395	5506 ± 455
	drug [N^+]	0	588 ± 84	2300 ± 250
	total [N^+][c]	6552 ± 609	6706 ± 479	7806 ± 706
kidney	native [N^+]	4115 ± 296	3251 ± 149	1560 ± 474
	drug [N^+]	0	2176 ± 192	5034 ± 1060
	total [N^+]	4115 ± 296	5427 ± 340	6594 ± 1534

[a] Total dose: 20 mg/kg/day × 5 days → 100 mg/kg (215.3 μmol/kg). [b] Total dose:15 mg/kg/day × 6 days → 90 mg/kg (208.3 μmol/kg). [c] Total [N^+] equivalents = 2[diamine] + 3[triamine] + 4[tetraamine]. Values expressed as nequiv of [N^+]/g of wet weight.

quences of these polyamine levels on the net polyamine [N^+] equivalents present in each tissue are depicted in Table 4.

The lack of accumulation of the dideethylated metabolite from $(HO)_2$DEHSPM is best illustrated in Table 5, which analyzes the data from the perspective of mass balance of the cumulative dose, i.e., how much of the original total dose remains in the liver and kidney and what form is it in, parent drug or metabolite? A 30 g mouse would have received a cumulative dose of 2.7 mg (6.25 μmol) of DEHSPM or 3.0 mg (6.46 μmol) of $(HO)_2$DEHSPM. One day after cessation of treatment, 33.8% (2.11 μmol) of the original dose of DEHSPM can be accounted for in liver and kidneys. However, only a small portion, 5.0% (or 0.311 μmol), of the original dose is present in the form of unchanged parent drug; 28.8%, or 1.80 μmol, of the total original dose remains in these organs in the form of the dideethylated metabolite, HSPM. In $(HO)_2$DEHSPM-treated animals, a similar amount (6.96% of dose, or 0.450 μmol) of unmetabolized parent drug is present in liver and kidneys 24 h after cessation of treatment, but only 3.03% of the original dose is present in the form of the dideethylated metabolite, $(HO)_2$HSPM. In each tissue the amount of parent drug exceeds that of the metabolite, reflecting the lack of accumulation of $(HO)_2$HSPM.

Acute Toxicity. The acute toxicity of $(HO)_2$DEHSPM was assessed after ip administration of a single dose of 325 mg/kg to a group of five female CD-1 mice. Three of the five animals died in this experiment, suggesting that the acute toxicity of $(HO)_2$DEHSPM is similar to that of DEHSPM (LD_{50} = 325 mg/kg)[17] and DENSPM (LD_{50} = 325 mg/kg).[18]

Chronic Toxicity. In comparing the chronic toxicity of DEHSPM with that of $(HO)_2$DEHSPM, we elected not to use historical controls. The chronic LD_{50} for DEHSPM was determined to be 38 mg/kg/day × 5 days in this study. This value confirms the LD_{50} value we had previously reported.[17] No deaths were observed in groups of six animals each at $(HO)_2$DEHSPM doses of 20, 40, and 60 mg/kg/day × 5 days, so experiments were initiated at higher doses (no. of deaths/no. of animals): 70 (0/5), 80 (0/5), 90 (0/10), 100 (1/5), and 120 (2/5) mg/kg/day × 5 days. These data indicate an LD_{40} for $(HO)_2$DEHSPM of 120 mg/kg/day × 5 days. We estimate the LD_{50} to be 130 mg/kg based on the slope of the toxicity curve. These data establish $(HO)_2$DEHSPM to be at least 3 times less toxic in this chronic treatment regimen than its analogue DEHSPM. While the lower doses of $(HO)_2$DEHSPM did not cause deaths, animals did exhibit signs of toxicity. At 90 mg/kg for 5 days, the animals all exhibited lethargy, poor coat condition, and decreased, ataxic movements. The animals in this $(HO)_2$DEHSPM-treated group lost between 20% and 30% of their body weight (data not shown) but recovered in a period of 20 days after the dosing regimen. This was in contrast to DEHSPM-treated animals wherein a 20% loss of body weight was a sign of imminent death. Several severely affected $(HO)_2$DEHSPM-treated animals were necropsied. It was noted that the stomachs of these animals appeared herniated and were extremely distended with food. This suggests that this compound potently blocks gastric emptying.

Prevention of Castor Oil-Induced Diarrhea. The dosage of DEHSPM administered to the rats in this study (5 mg/kg) is equivalent to the clinically used dose of 30 mg/m^2 in humans. At this dosage DEHSPM effectively prevented the onset of diarrheal stooling for the 6 hour time period of the assay in this castor oil-induced diarrhea rat model. At the same dose of 5 mg/kg, $(HO)_2$DEHSPM was as effective as DEHSPM at preventing diarrhea. In addition, the body weight loss for each group was very similar. Neither group exhibited any diarrheal stooling during the assay. This suggests that $(HO)_2$DEHSPM could be an effective antidiarrheal agent for clinical use. The dose−response relationship shows, as expected, the higher dose of 18 mg/kg $(HO)_2$DEHSPM effectively prevented the onset of diarrhea but indicated that 5 mg/kg $(HO)_2$DEHSPM was the minimum effective dose for prevention of diarrhea in this assay. At 2.5 mg/kg, $(HO)_2$DEHSPM was partially effective, resulting in reduced stool output (Figure 8a) and maintenance of body weight (Figure 8b), although some diarrhea did occur within the 6 h observation period. At 1 mg/kg, $(HO)_2$DEHSPM was not an effective antidiarrheal.

Although the onset of diarrhea was slightly delayed relative to control rats and the total weight of stool output was somewhat less, the norspermine analogues, DENSPM and DPNSPM, even at doses of 40 and 15 mg/kg, respectively, were far less active as antidiarrheal compounds. Data for both stool output (Figure 1a) and weight loss (Figure 1b) clearly illustrate the similarity between DEHSPM and $(HO)_2$DEHSPM and their differences from DENSPM, DPNSPM, and HSPM.

Discussion

On the basis of animal studies in rodents and dogs, we must anticipate the possibility for toxicity as patients receive more chronic dosage regimens of DEHSPM in the treatment of chronic, severe ARD. Thus our central goal was to develop a less toxic polyamine with similar potency to DEHSPM as an antidiarrheal. Since the HSPM backbone appeared to be required for potent antidiarrheal activity, our strategy was to render these terminal aminobutyl segments susceptible to further metabolic degradation without significantly altering the nonmetabolic biological properties of the DEHSPM pharmacophore. Thus while $(HO)_2$DEHSPM is indeed more highly substituted than DEHSPM, it nevertheless maintains enough structural similarity to DEHSPM to be "read" by L1210 cells as DEHSPM. First, the abilities of $(HO)_2$DEHSPM and DEHSPM to compete with radiolabeled spermidine for transport into L1210 cells were found to be essentially identical, just as computer-assisted molecular modeling had predicted. HPLC analysis of L1210 cells grown for 48 h in the presence of analogue showed that at an intracellular concentration of ca. 3 mM, each analogue had a very similar effect on intracellular native polyamine pools. Finally, $(HO)_2$DEHSPM and DEHSPM have the same

Table 5. Amount[a] (%) of Total Dose Present in Liver and Kidney

	treatment	unmetabolized parent drug, DEHSPM/$(HO)_2$DEHSPM (μmol)	dideethylated metabolite, HSPM/$(HO)_2$HSPM (μmol)	total drug + metabolite (μmol)
liver	DEHSPM[b]	0.115 (1.84 ± 0.53%)	1.394 (22.30 ± 2.10%)	1.509 (24.15%)
	$(HO)_2$DEHSPM[c]	0.219 (3.39 ± 0.48%)	0.166 (2.57 ± 0.38%)	0.385 (5.96%)
kidneys	DEHSPM[b]	0.196 (3.14 ± 1.37%)	0.408 (6.53 ± 0.67%)	0.604 (9.67%)
	$(HO)_2$DEHSPM[c]	0.231 (3.57 ± 0.34%)	0.030 (0.47 ± 0.01%)	0.261 (4.04%)
both tissues	DEHSPM[b]	0.311 (4.98%)	1.802 (28.83%)	2.113 (33.82%)
	$(HO)_2$DEHSPM[c]	0.450 (6.96%)	0.196 (3.03%)	0.646 (10.01%)

[a] Mass balance accounting for fate of the total orginal dose normalized for a 30 g mouse. [b] Total dose = 15 mg/kg/day × 6 days = 90 mg/kg → 2.7 mg (6.25 μmol) for a 30 g mouse. [c] Total dose = 20 mg/kg/day × 5 days = 100 mg/kg → 3.0 mg (6.46 μmol) for a 30 g mouse.

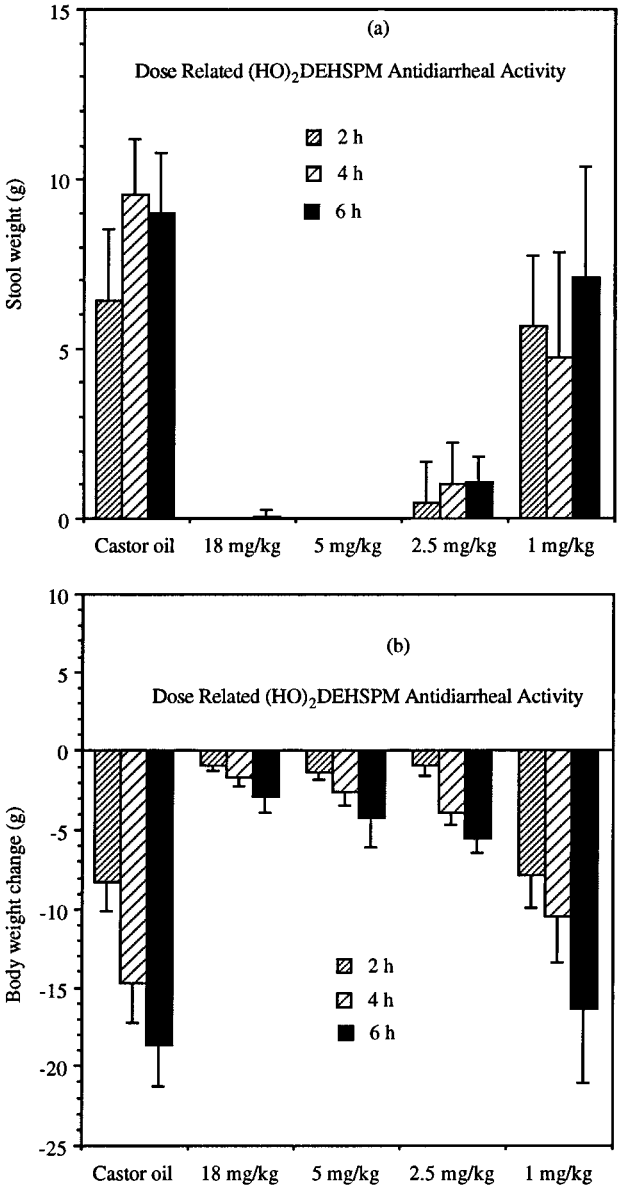

Figure 8. Antidiarrheal dose−response for $(HO)_2$DEHSPM in the rat castor oil-induced diarrheal model. Drug was administered as an sc injection followed, after 30 min, by gastric gavage of castor oil (5 mL/kg). Stool output (a) and body weight loss (b) were measured at 2, 4, and 6 h. The mininum effective dose for $(HO)_2$DEHSPM was 5 mg/kg. Data are not corrected for slight evaporative losses that occur during the assay. Such corrections do not significantly affect the results.

effect on L1210 cell growth, with nearly identical 48 and 96 h dose−effect curves.

Tetraamines are only poorly exported from cells unless acetylated,[26] and the cytosolic acetylase SSAT only recognizes aminopropyl moieties with a primary amino terminus as substrates.[27] Thus the first requirement to enable metabolic clearance of terminal diethyltetraamine analogues is *N-deethylation* to provide a primary amine terminus. It is interesting to note that under our *in vitro* conditions, L1210 cells apparently do not *N*-deethylate either $(HO)_2$DEHSPM or DEHSPM to any significant extent. In contrast, tissues examined from animals (mouse, rat, dog) treated with DENSPM,[18] DEHSPM,[17] or $(HO)_2$DEHSPM do contain N-deethylated metabolites, thus meeting the first requirement of SSAT for a primary amine terminus. However, if the second criterion of an exposed aminopropyl segment is not met, further degradation via the SSAT/PAO pathway is precluded. Thus HSPM, a tetraamine comprised exclusively of aminobutyl segments, can neither be further degraded nor exported from the cell, resulting in its accumulation. We postulated that this accumulation and persistent retention of HSPM was responsible for the markedly greater toxicity (5-fold) of DEHSPM vs DENSPM when administered chronically, even though the acute toxicities of DENSPM and DEHSPM are essentially identical.[17,18] Therefore the design concept was to modify the polyamine backbone of DEHSPM in such a manner as to render the aminobutyl segments susceptible to further metabolic transformation and clearance.

We elected to introduce hydroxy groups into the external aminobutyl segments of DEHSPM in a position and configuration analogous to the (*R*)-(−)-2-hydroxyputrescine segment of (+)-hypusine.[23] The rat liver is able to convert 2-hydroxyputrescine itself to γ-amino-β-hydroxybutyric acid.[28] Thus, we hoped that enzymes involved in 2-hydroxyputrescine and/or hypusine metabolism or perhaps other enzyme systems present in normal tissues might be able to degrade or otherwise facilitate elimination of the tetraamine. Possibilities could include, for example: (1) direct conjugation of the OH to make the molecule exportable and excretable, e.g., glucuronidation, or (2) oxidation at the hydroxyl-bearing carbon by either (a) a constitutive enzyme system normally functioning in hypusine metabolism, or (b) some other more 'nonspecific' oxidase/dehydrogenase to result in cleavage of the external aminobutyl segments. While we do not yet have any evidence as to which of these or other degradative mechanisms is operating, it is clear that there is no significant accumulation of $(HO)_2$HSPM. One day after a chronic treatment regimen, only 10% of the total dose of $(HO)_2$DEHSPM remains in liver and kidney compared with 34% of the total DEHSPM dose. In both liver and kidney, DEHSPM had significantly disrupted normal tissue polyamine homeostasis as indicated by the effects on native polyamine pools and total $[N^+]$ equivalents ('net charge balance'). In contrast equimolar treatment with $(HO)_2$DEHSPM had no significant impact on polyamine homeostasis in the liver, and while there was

some impact on the kidney, it was mild compared to that of DEHSPM. These results support our view that the degree of tetraamine buildup and its duration are responsible for a substantial portion of the toxicity that can occur with DEHSPM and explain the 3-fold decrease in chronic toxicity of $(HO)_2$DEHSPM compared to DEHSPM and thus validate the hydroxylated polyamine analogue design concept.

Conclusion

The data clearly support earlier findings that the critical issue in how the cell "reads" a polyamine analogue is very dependent on the molecule's charge and the separation between the charge centers.[29] Thus it is possible to operate on the methylene backbones, i.e., the insulators between charged centers, of these molecules, altering their metabolic properties while still maintaining the desired pharmacological activity. As we have demonstrated, *such metabolic programming can result in polyamine analogues with substantially reduced toxicities.* Finally, it seems clear that the CoMFA profiles generated from our expanding library of polyamines are very useful in drug design by assessing whether a cell will recognize modified analogues, at least at the level of polyamine transport. These modifications in the backbone can be made while still maintaining the desired pharmacological properties.

Experimental Section

Chemical reagents were purchased from Aldrich Chemical Co. Reactions using hydride reagents were run in distilled DMF or THF (from sodium and benzophenone) under a nitrogen atmosphere. Fisher Optima grade solvents were routinely used, and organic extracts were dried with sodium sulfate. Silica gel 32−63 (40 μM "flash") from Selecto, Inc. (Kennesaw, GA) was used for column chromatography. Melting points were determined on a Fisher-Johns melting point apparatus and are uncorrected. Proton NMR spectra were run at 300 MHz in $CDCl_3$ (not indicated) or D_2O with chemical shifts given in parts per million downfield from tetramethylsilane or 3-(trimethylsilyl)propionic-*2,2,3,3-d*$_4$ acid, sodium salt, respectively. Coupling constants (J) are in hertz. FAB mass spectra were run in a *m*-nitrobenzyl alcohol matrix. Elemental analyses were performed by Atlantic Microlabs, Norcross, GA.

Computer Modeling. A series of *N*-alkylated polyamines, terminally dialkylated analogues and homologues of spermine which have been synthesized by methods developed in these laboratories,[29−31] were used to generate the CoMFA analysis. The structures and K_i values, both calculated and actual, for the polyamine uptake apparatus of these polyamine analogues are listed in Table 1.

On the basis of pK_a values measured[29] for DENSPM (**11**), DESPM (**15**), DEHSPM (**20**), FDESPM (**17**), PIP(4,4,4) (**29**), PYR(4,4,4) (**30**), and PIP(5,4,5) (**31**) (Table 1), we have made the following assumptions about the protonation state. All of the nonaromatic tetraamines are largely in the form of the tetracation at physiological pH 7.2. The spermine analogues **13**−**16** and **34** and the homospermine analogues and homologues **18**−**26**, **29**, and **31**−**33** should be 85% and 97%, respectively, in the form of the tetracations. The norspermine analogues **9**−**12** and **27** should be at least 74% in the form of the tetracations. Compounds **17** and **30** should be almost exclusively in the form of the internal dication at physiological pH. Compound **28** should also be a dication, but because of resonance it should be a terminal dication. Thus the calculation of atomic charges and the conformational search of these analogues were carried out based on the anticipated protonated structures.

The low-energy conformations of polyamine analogues were obtained by systematic conformational searching supported by Tripos Associates, Inc. in SYBYL 6.02 molecular modeling program.[19] The CoMFA were performed using the QSAR option of SYBYL 6.02 program running on a Silicon Graphics Indigo2 workstation.

The energies of steric and electrostatic interaction between each of the analogues were calculated as parameters, and a probe atom was placed at the various intersections of a regular 3D lattice, large enough to include all of the analogues in the database and with a 2.0 Å lattice space. The probe atom had the shape of sp^3 carbon and a charge of +1.0. The van der Waals values were taken from the standard Tripos force field, and the atomic charges were calculated by the method of Gasteiger and Marsili.[20] Wherever the probe atom experiences a steric repulsion greater than "cutoff" (30 kcal/mol in these studies), the steric interaction is set to the value "cutoff", and the electrostatic interaction was set to the mean of the other molecular electrostatic interactions at the same location. The resulting steric and electrostatic field values, on a regularly spaced lattice around the analogues, were then correlated with the K_i data for the polyamine transport system by a very efficient statistical method, partial least squares (PLS).[21] Statistical techniques, bootstrapping, and cross-validation are used to determine the quality of the correlation.[21,22] The cross-validation technique involves random elimination of one or more analogues from the original data set with subsequent equation development and activity prediction for the eliminated analogues in an interactive manner, thus yielding a QSAR equation that is generally of greater predictive value than that derived from conventional regression analysis. The implementation of PLS also rotates the PLS solution back into the original data space, thus generating a "conventional" QSAR equation showing *r*-square, *F* test, and the standard error *S*.

The initial alignment of the molecules, the positioning of a molecular model within the fixed lattice, is by far the most critical step in developing a successful CoMFA model, since the relative interaction energies depend strongly on relative molecular positions. In this series of molecules, both the end nitrogen atoms of the analogues and the third nitrogen atom were finally found as atom pairs between two molecules for performing a best fit and then followed again by energy minimization using the standard Tripos force field option, and the resulting structures were used to generate the CoMFA analysis. DESPM (**15**) was chosen as the template in the alignment of polyamine analogues.

Cell Culture. Murine L1210 leukemia cells were maintained in logarithmic growth as a suspension culture in RPMI-1640 medium containing 10% FBS, 2% HEPES-MOPS buffer, 1 mM aminoguanidine, and 1 mM L-glutamine (Sigma) at 37 °C in a water-jacketed 5% CO_2 incubator.

IC_{50} Determinations. Cells were grown in 25 cm^2 tissue culture flasks in a total volume of 10 mL and treated while in logarithmic growth ($0.5-1.0 \times 10^5$ cells/mL) with polyamine derivatives dissolved in sterile water and filtered through a 0.2 μm filter. For the 96 h IC_{50} determinations, cells were reseeded after 48 h and incubated for an additional 48 h. Cells were routinely counted electronically (Model Z_F Coulter counter, Coulter Electronics, Hialeah, FL) with this result confirmed periodically by a hemocytometer. The percentage of control growth was calculated as follows:

$$\% \text{ of control growth} = \left(\frac{\text{final treated cell no.} - \text{initial inoculum}}{\text{final untreated cell no.} - \text{initial inoculum}}\right) \times 100$$

The IC_{50} is defined as the concentration of compound necessary to reduce cell growth to 50% of control growth after defined intervals of exposure.

Polyamine Pool Analysis. Cells in logarithmic growth were treated with the polyamine derivatives. At the end of the treatment period, cell suspensions were washed twice with cold medium (RPMI-1640) and homogenized in 0.6 N perchloric acid.[32] This homogenate was stored frozen at −80 °C until analysis by HPLC.

K_i Determinations. The polyamine derivatives were studied for their ability to compete with [^{3}H]SPD or [^{14}C]SPD uptake into L1210 leukemia cells *in vitro*.[32] Cell suspensions were incubated in 1 mL of RPMI-1640 containing 1, 2, 4, 6, 8,

and 10 μM radiolabeled SPD alone or with the additional presence of 10, 25, and 50 μM polyamine analogue for 20 min at 37 °C. At the end of the incubation period, tubes were centrifuged at 900*g* for 5 min at 0−4 °C, and the pellet was washed twice with 5 mL of ice-cold RPMI-1640 containing 1 mM SPD. The washed pellet was dissolved in 200 μL of 1 N NaOH at 60 °C for 1 h, neutralized with 1 N HCl, and transferred to a vial for scintillation counting. Lineweaver−Burke plots indicated a simple competitive inhibition with respect to SPD [K_m(SPD) = 2.1 ± 0.2 μM].

NMDA Assay. The procedure for assaying specific binding of [^{3}H]MK-801 to the *N*-methyl-D-aspartate receptor complex was a modification of the method of Ransom and Stec.[33] Cerebral cortices from young male Sprague−Dawley rats (200−300 g) were homogenized with 10 vol of ice-cold 0.32 M sucrose using a motor-driven glass/Teflon homogenizer. The homogenate was centrifuged at 1000*g* for 10 min, and the pellet was discarded. The supernatant was then centrifuged at 18000*g* for 20 min. The 18000*g* pellet was then resuspended in 10 vol of buffer A (5 mM Tris-HCl, pH 7.7) at 4 °C, homogenized using high-intensity ultrasound, and centrifuged at 8000*g* for 20 min. The supernatant and upper buffy coat of the pellet were combined and centrifuged at 50000*g* for 20 min. The pellet was then resuspended in 10 vol of buffer A and homogenized using high-intensity ultrasound. These resuspended membranes were then centrifuged at 50000*g*, discarding the supernatant. The membranes were washed in this manner an additional three times and stored as a frozen suspension at −80 °C for at least 18 h but no longer than 2 weeks before use.

For binding experiments, frozen membranes were thawed, pelleted at 50000*g* for 20 min, and washed as described above, except that 20 vol of buffer A was used for resuspension, for a total of four times. The final pellet was resuspended in buffer B (5 mM Tris-HCl, pH 7.5, 23 °C). The binding assay mixture was 1.00 mL of buffer B containing 200−300 μg of membrane protein (Lowry method[34]), 100 μM L-glutamate, 100 μM glycine, 2 nM [^{3}H]MK-801, and tetraamine at the following concentrations: 0 ("100% + L-Glu + Gly control") and 0.05, 0.1, 0.5, 1, 5, 10, 50, 100, 500, and 1000 μM. Nonspecific binding was determined using 100 μM MK-801. Binding assays were performed in triplicate at 23 °C for 1 h and terminated by filtration through Whatman GF/B glass fiber filters followed by three 4.0 mL rinses of ice-cold buffer B using a Brandel M-48 Cell Harvester.

Metabolism of (HO)$_2$DEHSPM vs DEHSPM in Mouse Liver and Kidney. Groups of three female CD-1 mice received a subchronic treatment regimen of either (a) a total dose of 100 mg/kg (216 μmol/kg) (HO)$_2$DEHSPM or (b) a total dose of 90 mg/kg (208 μmol/kg) DEHSPM. Animals were sacrificed for HPLC analysis 1 day after the final dose.

HPLC Analysis of Polyamines in Mouse Tissues. Various tissues including the liver and kidney were prepared for HPLC analysis of polyamine content. In order to facilitate their handling, the organs were frozen in liquid nitrogen, weighed, and homogenized (Tissuemizer, Tekmar, Cincinnati, OH) in 1.2 N perchloric acid (containing 1,7-diaminoheptane internal standard) in a 1:20 (w/v) ratio. The tissue homogenates were then freeze−thawed three times and stored in a −70 °C freezer until HPLC analysis was performed.

Each chromatographic assay included calibration standards which were treated in the same manner as the samples. The calibration standards (typical retention times in minutes are indicated) were prepared by adding known amounts of PUT (9.63), 1,6-diaminohexane (13.04), 1,7-diaminoheptane (15.39), SPD (20.88), (HO)$_2$HSPM (24.28), SPM (26.75), HSPM (27.60), (HO)$_2$DEHSPM (28.37), MEHSPM (29.80), and DEHSPM (31.85) to a matrix that resembled the sample matrix. The concentration of each polyamine was calculated from the peak area by calibration curves obtained by nonweighted least-squares linear regression. Peak area and linear regression calculations were performed on a Macintosh Centris 650 instrument with Rainin Dynamax HPLC Method Manager software (Rainin Instrument Co., Ridgefield, NJ). The method had a detection limit ≤ 0.1 nmol/mL and was reproducible and linear over the range 0.5−100 nmol/mL.

Acute and Chronic Toxicity of Polyamine Analogues in Mice. For acute toxicities, the polyamine analogues were administered as a single ip injection. The animals were scored 2 h after administration of drug. All survivors were observed for a period of 10 days after the treatment. In the chronic toxicity regimen, mice were administered the polyamine analogue as 1 ip dose/day for 5 days. Body weight and observations of coat health and overall physical appearance were recorded at the time of each injection. After the treatment regimen had been completed, animals were examined daily for an additional 10 days. The chronic toxicity dosing regimen was set up so that at least one test group presented with a high fraction of lethalities.

Castor Oil-Induced Diarrhea. Male Sprague−Dawley rats (350−400 g) were fasted overnight in hanging wire cages and allowed free access to water. A typical experiment involved 12 rats: six untreated controls and six pretreated with polyamine analogues (sc injection 30 min prior to castor oil). All animals were then challenged with castor oil[35] (gastric gavage of 1 mL/200 g of body weight) at $T = 0$ and monitored for a 6 h period during which they received no food or water. Onset of diarrhea for the control rats was between 30 and 90 min and lasted for at least 6 h. Time of diarrheal onset was recorded for each animal in the control and treated groups, and the animal weight and stool weight were recorded at 2, 4, and 6 h.

4,9-Dibenzyl-1,12-dichloro-(2*S*),(11*S*)-dihydroxy-4,9-diazadodecane (2). $MgSO_4$ (5 g) was added to a solution of **1**[24] (5.45 g, 20.3 mmol) and (*S*)-(+)-epichlorohydrin (4.13 g, 44.7 mmol) in distilled methanol (120 mL). The reaction mixture was stirred at room temperature for 2 days until completion of the reaction as monitored by TLC. The solid was filtered, and the filtrate was concentrated *in vacuo* to leave an oil. Flash chromatography with 80/15/5 hexane/EtOAc/EtOH afforded 6.23 g (68%) of **2** as an oil: NMR δ 1.40 (m, 4 H), 2.50 (m, 8 H), 3.50 (m, 4 H), 3.56 (dd, 4 H, J = 25.6, 1.2), 3.80 (m, 2 H), 7.27 (m, 10 H). Anal. ($C_{24}H_{34}Cl_2N_2O_2$) C, H, N.

4,9-Dibenzyl-1,12-dicyano-(2*R*),(11*R*)-dihydroxy-4,9-diazadodecane (3). A mixture of **2** (2.91 g, 6.4 mmol), KCN (4.18 g, 64 mmol), and 18-crown-6 (0.17 g, 0.64 mmol) in dry acetonitrile (80 mL) was heated at 60 °C for 2 days. The solid was filtered, and the solvent was removed by rotary evaporation. The residue was purified using flash column chromatography with 60/35/5 hexane/EtOAc/EtOH to afford a solid, which was recrystallized from 30/70 CH_2Cl_2/hexane to furnish 1.8 g (65%) of **3** as a white solid: mp 85 °C; NMR δ 1.46 (m, 4 H), 2.48 (m, 12 H), 3.60 (dd, 4 H, J = 24.2, 4.5), 3.73 (m, 2 H), 7.29 (m, 10 H). Anal. ($C_{26}H_{34}N_4O_2$) C, H, N.

***N*^{5},*N*^{10}-Dibenzyl-(3*R*),(12*R*)-dihydroxyhomospermine (4).** W-2 grade Raney nickel (0.7 g) was added to a solution of **3** (1.42 g, 3.04 mmol) in methanol (100 mL) in a 500 mL Parr bottle, and a slow stream of NH_3 was bubbled through the mixture for 20 min at 0 °C. Hydrogenation was carried out with shaking at 50 psi for 7 h. The suspension was filtered through Celite, and the solvents were evaporated *in vacuo* to afford 1.12 g (86%) of **4** as an oil: NMR δ 1.41 (m, 4 H), 2.42 (m, 8 H), 2.82 (m, 8 H), 3.55 (d, 4 H, J = 2.6), 3.71 (m, 2 H), 7.52 (m, 10 H); HRMS calcd for $C_{26}H_{42}N_4O_2$ 443.3386 (M + 1), found 443.3383 (M + 1).

(3*R*),(12*R*)-Diacetoxy-*N*^{1},*N*^{14}-diacetyl-*N*^{5},*N*^{10}-dibenzylhomospermine (5). A solution of **4** (2.4 g, 5.42 mmol) in CH_2Cl_2 (100 mL) was treated with acetic anhydride (10 mL) at room temperature for 3 h. The volatiles were evaporated *in vacuo*, and the concentrate was purified by flash chromatography with 65/25/15 hexane/EtOAc/EtOH to give 2.39 g (73%) of **5** as an oil: NMR δ 1.44 (m, 4 H), 1.96 (m, 3 H), 1.98 (m, 4 H), 2.07 (s, 3 H), 2.46 (m, 8 H), 2.57 (m, 2 H), 3.02 (m, 2 H), 3.42 (m, 2 H), 3.59 (m, 4 H), 7.28 (m, 10 H). Anal. ($C_{34}H_{50}N_4O_6$) C, H, N.

***N*^{5},*N*^{10}-Dibenzyl-*N*^{1},*N*^{14}-diethyl-(3*R*),(12*R*)-dihydroxyhomospermine (6).** $LiAlH_4$ (1 M in THF, 15 mL, 15 mmol) was added to a solution of **5** (1.73 g, 2.83 mmol) in dry THF (50 mL). The mixture was stirred at 65 °C for 3 h under N_2. The reaction was cautiously quenched with water (5 mL) followed by filtration of the solids. Evaporation of the filtrate and flash chromatography on silica gel, eluting with 5% concentrated NH_4OH in methanol, produced 0.6 g (44%) of **6**

as an oil: NMR δ 1.09 (m, 6 H), 1.47 (m, 8 H), 2.64 (m, 16 H), 3.59 (m, 4 H), 3.75 (m, 2 H), 7.28 (m, 10 H). Anal. ($C_{30}H_{50}N_4O_2$) C, H, N.

***N*^{1},*N*^{14}-Diethyl-(3*R*),(12*R*)-dihydroxyhomospermine Tetrahydrochloride [(HO)$_2$DEHSPM] (7).** Pd−C (10%, 0.4 g) was added to a solution of **6** (2.26 g, 4.53 mmol) in concentrated HCl (3 mL) and EtOH (100 mL), and the suspension was degassed three times with N_2. After stirring under hydrogen (1 atm, 3 h), the catalyst was filtered off and washed with water (10 mL). The solvents were removed under reduced pressure to give a white solid. Recrystallization from aqueous EtOH gave 1.5 g (72%) of **7** as a crystalline solid: NMR (D_2O) δ 1.07 (t, 6 H, J = 2.4), 1.60 (m, 4 H), 1.74 (m, 4 H), 2.91 (m, 16 H), 3.84 (m, 2 H). Anal. ($C_{16}H_{42}Cl_4N_4O_2$) C, H, N.

(3*R*),(12*R*)-Dihydroxyhomospermine Tetrahydrochloride [(HO)$_2$HSPM] (8). HCl (1 N, 10 mL) and 10% Pd−C (0.08 g) were added to a solution of **4** (0.764 g, 1.73 mmol) in methanol (100 mL), and the suspension was flushed three times with nitrogen. The mixture was exposed to hydrogen for 3 h at atmospheric pressure followed by filtration of catalyst on Celite. The filtrate was evaporated *in vacuo* to give a white solid. Recrystallization from aqueous ethanol produced 0.56 g (80%) of **8** as a crystalline solid: NMR (D_2O) δ 1.63 (m, 8 H), 2.97 (m, 12 H), 3.92 (m, 2 H). Anal. ($C_{12}H_{34}Cl_4N_4O_2$) C, H, N.

Acknowledgment. Financial support was provided by SunPharm Corp., Jacksonville, FL, and National Institutes of Health, Grant No. CA37606.

References

(1) Gillin, J. S.; Shike, M.; Alcock, N.; Urmacher, C.; Krown, S.; Kurtz, R. C.; Lightdale, C. J.; Winawer, S. J. Malabsorption and Mucosal Abnormalities of the Small Intestine in the Acquired Immunodeficiency Syndrome. *Ann. Intern. Med.* **1985,** *102*, 619−622.

(2) Chandrasekar, P. H. "Cure" of Chronic Cryptosporidiosis During Treatment with Azidothymidine in a Patient with the Acquired Immune Deficiency Syndrome. *Am. J. Med.* **1987,** *83*, 187.

(3) Simon, D.; Weiss, L.; Tanowitz, H. B.; Wittner, M. Resolution of *Cryptosporidium* Infection in an AIDS Patient after Improvement of Nutritional and Immune Status with Octreotide. *Am. J. Gastroenterol.* **1991,** *86*, 615−618.

(4) Abrams, D. I.; Goldman, A. I.; Launer, C.; Korvick, J. A.; Neaton, J. D.; Crane, L. R.; Grodesky, M.; Wakefield, S.; Muth, K.; Kornegay, S.; Cohn, D. L.; Harris, A.; Luskin-Hawk, R.; Markowitz, N.; Sampson, J. H.; Thompson, M.; Deyton, L. A Comparative Trial of Didanosine or Zalcitabine after Treatment with Zidovudine in Patients with Human Immunodeficiency Virus Infection. *N. Engl. J. Med.* **1994,** *330*, 657−662.

(5) Lopez, A. P.; Gorbach, S. L. Diarrhea in AIDS. *Infect. Dis. Clin. North Am.* **1988,** *2*, 705−718.

(6) Antony, M. A.; Brandt, L. J.; Klein, R. S.; Bernstein, L. H. Infectious Diarrhea in Patients with AIDS. *Dig. Dis. Sci.* **1988,** *33*, 1141−1146.

(7) Simon, D.; Weiss, L. M.; Brandt, L. J. Treatment Options for AIDS-Related Esophageal and Diarrheal Disorders. *Am. J. Gastroenterol.* **1992,** *87*, 274−281.

(8) Grosman, I.; Simon, D. Potential Gastrointestinal Uses of Somatostatin and Its Synthetic Analogue Octreotide. *Am. J. Gastroenterol.* **1990,** *85*, 1061−1072.

(9) Farthing, M. J. G. Octreotide in the Treatment of Refractory Diarrhea and Intestinal Fistulae. *Gut* **1994**, *35* Suppl. 3, S5−10.

(10) Powell, D. W.; Szauter, K. E. Nonantibiotic Therapy and Pharmacotherapy of Acute Infectious Diarrhea. *Gastroenterol. Clin. North Am.* **1993**, *22*, 683−707.

(11) Tansy, M. F.; Martin, J. S.; Landin, W. E.; Kendall, F. M.; Melamed, S. Spermine and Spermidine as Inhibitors of Gastrointestinal Motor Activity. *Surg. Gynecol. Obstet.* **1982,** *154*, 74−80.

(12) Melamed, S.; Carlson, G. R.; Moss, J. N.; Belair, E. J.; Tansy, M. F. GI Pharmacology of Polyethyleneimine I: Effects on Gastric Emptying in Rats. *J. Pharm. Sci.* **1977,** *66*, 899−901.

(13) Tansy, M. F.; Martin, J. S.; Innes, D. L.; Kendall, F. M.; Melamed, S.; Moss, J. N. GI Pharmacology of Polyethyleneimine II: Motor Activity in Anesthetized Dogs. *J. Pharm. Sci.* **1977**, *66*, 902−904.

(14) Belair, E. J.; Carlson, G. R.; Melamed, S.; Moss, J. N.; Tansy, M. F. Effects of Spermine and Spermidine on Gastric Emptying in Rats. *J. Pharm. Sci.* **1981,** *70*, 347.

(15) Sato, T. L.; Sninsky, C. A.; Bergeron, R. J. Structural Specificity of Synthetic Analogues of Polyamines and their Effect on Gastrointestinal Motility. In *Polyamines and the gastrointestinal tract, Falk Symposium No. 62*; Dowling, R. H., Folsch, U. R., Loser, C., Eds.; Kluwer Academic Publishers: Boston, MA, 1991.

(16) Sninsky, C. A.; Bergeron, R. Potent Anti-Diarrheal Activity of a New Class of Compounds: Synthetic Analogs of the Polyamine Pathway. *Gastroenterology* **1993**, *104*, A584.

(17) Bergeron, R. J.; Weimar, W. R.; Luchetta, G.; Sninsky, C. A.; Wiegand, J. Metabolism and Pharmacokinetics of *N*^{1},*N*^{14}-Diethylhomospermine. *Drug Metab. Dispos.* **1995,** *23*, 334−343.

(18) Bergeron, R. J.; Weimar, W. R.; Luchetta, G.; Streiff, R. R.; Wiegand, J.; Perrin, J.; Schreier, K. M.; Porter, C.; Yao, G. W.; Dimova, H. Metabolism and Pharmacokinetics of *N*^{1},*N*^{11}-Diethylnorspermine. *Drug Metab. Dispos.* **1995,** *23*, 1117−1125.

(19) SYBYL, Version 602, Tripos Associates, Inc., St. Louis, MO; July 21, 1993.

(20) Gasteiger, J.; Marsili, M. Interactive Partial Equalization of Orbital Electronegativity-A Rapid Access to Atomic Charges. *Tetrahedron* **1980**, *36*, 3219−3228.

(21) Cramer, R. D., III; Bunce, J. D.; Petterson, D. E.; Frank, I. E. Crossvalidation, Bootstrapping, and Partial Least Squares Compared with Multiple Regression in Conventional QSAR Studies. *Quant. Struct.-Act. Relat. Pharmacol. Chem. Biol.* **1988**, *7*, 18−25.

(22) Wold, S. Cross-validatory Estimation of the Number of Components in Factor and Principal Components Models. *Technometrics* **1978**, *20*, 397−405.

(23) Bergeron, R. J.; Xia, M. X. B.; Phanstiel, O., IV. Total Synthesis of (+)-Hypusine and Its (2*S*,9*S*)-Diastereomer. *J. Org. Chem.* **1993**, *58*, 6804−6806.

(24) Samejima, K.; Takeda, Y.; Kawase, M.; Okada, M.; Kyogoku, Y. Synthesis of ^{15}N-Enriched Polyamines. *Chem. Pharm. Bull.* **1984**, *32*, 3428−3435.

(25) Bergeron, R. J.; Weimar, W. R.; Wu, Q.; Austin, J. K., Jr.; McManis, J. S. Impact of Polyamine Analogues on the NMDA Receptor. *J. Med. Chem.* **1995,** *38*, 425−428.

(26) Pegg, A. E.; Wechter, R.; Pakala, R.; Bergeron, R. J. Effect of *N*^{1},*N*^{12}-Bis(ethyl)spermine and Related Compounds on Growth and Polyamine Acetylation, Content, and Excretion in Human Colon Tumor Cells. *J. Biol. Chem.* **1989**, *264*, 11744−11749.

(27) Seiler, N. Acetylation and Interconversion of the Polyamines. In *The Physiology of Polyamines*; Bachrach, U., Heimer, Y. M., Eds.; CRC Press: Boca Raton, FL, 1989; Vol. I, Chapter 11, pp 159−176.

(28) Nakao, J.; Hasegawa, T.; Hashimoto, H.; Noto, T.; Nakajima, T. Formation of GABOB from 2-Hydroxyputrescine and Its Anticonvulsant Effect. *Pharmacol. Biochem. Behav.* **1991**, *40*, 359−366.

(29) Bergeron, R. J.; McManis, J. S.; Weimar, W. R.; Schreier, K. M.; Gao, F.; Wu, Q.; Ortiz-Ocasio, J.; Luchetta, G. R.; Porter, C.; Vinson, J. R. T. The Role of Charge in Polyamine Analogue Recognition. *J. Med. Chem.* **1995**, *38*, 2278−2285.

(30) Bergeron, R. J.; McManis, J. S.; Liu, C. Z.; Feng, Y.; Weimar, W. R.; Luchetta, G. R.; Wu, Q.; Ortiz-Ocasio, J.; Vinson, J. R. T.; Kramer, D.; Porter, C. Antiproliferative Properties of Polyamine Analogues: A Structure-Activity Study. *J. Med. Chem.* **1994,** *37*, 3464−3476.

(31) Bergeron, R. J.; Neims, A. H.; McManis, J. S.; Hawthorne, T. R.; Vinson, J. R. T.; Bortell, R.; Ingeno, M. J. Synthetic Polyamine Analogues as Antineoplastics. *J. Med. Chem.* **1988**, *31*, 1183−1190.

(32) Bergeron, R. J.; Hawthorne, T. R.; Vinson, J. R. T.; Beck, D. E., Jr.; Ingeno, M. J. Role of the Methylene Backbone in the Antiproliferative Activity of Polyamine Analogues on L1210 Cells. *Cancer Res.* **1989**, *49*, 2959−2964.

(33) Ransom, R. W.; Stec, N. L. Cooperative Modulation of [^{3}H]MK-801 Binding to the *N*-Methyl-D-Aspartate Receptor-Ion Channel Complex by L-Glutamate, Glycine, and Polyamines. *J. Neurochem.* **1988,** *51*, 830−836.

(34) Lowry, O. H.; Rosebrough, N. J.; Farr, A. L.; Randall, R. J. Protein Measurement with the Folin Phenol Reagent. *J. Biol. Chem.* **1951,** *193*, 265−275.

(35) Eaker, E. Y.; Bixler, G. B.; Mathias, J. R. WHR 1049, a Potent Metabolite of Lidamidine, Has Antidiarrheal and Antimotility Effects on the Small Intestine in Rats. *J. Pharmacol. Exp. Ther.* **1988**, *246*, 786−789.

JM950827H